İSTANBUL TİCARET ÜNİVERSİTESİ
FEN BİLİMLERİ DERGİSİ

İstanbul Commerce University Journal of Science

http://dergipark.org.tr/ticaretfbd

Research Article / Araştırma Makalesi

STUDYING THE ELECTROCHEMICAL BEHAVIORS OF ANODIZED METALLIC IMPLANTS FOR IMPROVED CORROSION RESISTANCE

GELİŞMİŞ KOROZYON DİRENCİ İÇİN ELOKSALLI METALİK İMPLANTLARIN ELEKTROKİMYASAL DAVRANIŞLARININ İNCELENMESİ

Md. Shafinur MURAD[1] Aybala USTA[2] Ramazan ASMATULU[3] Muhammet CEYLAN[4]

https://doi.org/10.55071/ticaretfbd.1109393

Corresponding Author / Sorumlu Yazar
aybala.usta@marmara.edu.tr

Received / Geliş Tarihi
26.04.2022

Accepted / Kabul Tarihi
22.06.2022

Abstract

A study about long-term corrosion behavior of anodized and non-anodized Ti6Al4V and MgAZ31B biomaterials was conducted under controlled conditions. By applying 20V DC potential, MgAZ31B alloys was anodized in phosphoric acid and potassium hydroxide while Ti6Al4V alloys was anodized in phosphoric acid and oxalic acid. Long-term experiments were carried out by immersing them in deionized (DI) water, 3% NaCl and phosphate-buffered saline (PBS) solutions. The corrosion rate and pattern were measured by electrochemical analysis. Also, as a result of anodization, the natural oxide layer was observed on the material surface, thus the corrosion rate is reduced and the life of the biomaterial has been improved.

Keywords: Anodization, corrosion, electrochemical behavior, metallic biomaterials.

Öz

Eloksallı ve anodize edilmemiş Ti6Al4V ve Mg AZ31B biyomalzemelerinin korozyon davranışına ilişkin uzun vadeli bir araştırma, kontrollü koşullar altında gerçekleştirilmiştir. Ti6Al4V fosforik asit ve oksalik asit içinde anodize edilirken, Mg AZ31B fosforik asit ve potasyum hidroksit içinde 20V DC potansiyel uygulanarak anodize edilmiştir. %3 NaCl, fosfat tamponlu salin (PBS) ve deiyonize (DI) su çözeltilerine daldırılarak uzun süreli deneyler yapıldı. Korozyon hızı ve deseni elektrokimyasal analiz ile ölçülmüş ve anotlamanın malzeme yüzeyindeki doğal oksit tabakasını arttırdığı, korozyon hızını azalttığı ve biyomalzemenin ömrünü uzattığı gözlemlenmiştir.

Anahtar Kelimeler: Anotlama, elektrokimyasal davranış, korozyon, metalik biyomalzemeler.

[1]Wichita State University, Faculty of Engineering, Department of Mechanical Engineering, 1845 Fairmount, Wichita, USA. shafinurwsu@gmail.com, Orcid.org/0000-0002-5680-9859.

[2]Marmara University, Faculty of Engineering, Department of Mechanical Engineering, Maltepe, Istanbul, Türkiye. aybala.usta@marmara.edu.tr, Orcid.org/0000-0002-6895-3540.

[3]Wichita State University, Faculty of Engineering, Department of Mechanical Engineering, 1845 Fairmount, Wichita, USA. ramazan.asmatulu@wichita.edu, Orcid.org/0000-0001-8104-2285.

[4]İstanbul Commerce University, Faculty of Engineering,, Department of Mechatronics Engineering, Kücükyalı, İstanbul, Türkiye. mceylan@ticaret.edu.tr, Orcid.org/0000-0001-6933-2917.

1. INTRODUCTION

Among joint replacements operations, hip and knee replacement are the most commonly performed orthopedic surgeries in the US. According to a Mayo Clinic orthopedics study. 4.7 million US citizens have a knee replacement, and 2.5 million have a hip replacement (Maradit et al., 2014). Being able to use biomaterial implants in the human body, biomaterials must be biocompatible and should not have a harmful reaction (Bidhedi & Pouranvari, 2012). Biomaterial implants must endure the body's internal environment and have the strength to retain the critical period. Moreover, they are not supposed to degrade to a point where they cannot perform as expected. Second, a bioimplant should have high corrosive resistance to sustain enough mechanical strength over a long period. Polymer-based implants may have reduced mechanical efficiency and so have restricted applicability (Kumar et al., 2002; Uchi et al., 2001). In contrast to polymeric implants, metallic implants, which have been considered biomaterials and used in clinical trials since World War II (Manivasagam et al., 2010), exhibit better strength and resistance to fracture. In addition, because of the versatility of fabrication techniques, there is an increasing trend to replace deteriorated and destroyed biological components with metallic implants for artificial organs. However, on the other side, after the tissue has fully healed, it can release toxic ions necessitating a second surgical operation to be removed (Ferreira et al., 2003; Pietak et al., 2008; Rivera et al., 2008).

There have been various materials used in biomedical applications, such as polymers (Üner et al., 2012), ceramics, and metals (Hermawan et al., 2010); however, nowadays, metals are the most extensively used material in biomedical applications (Viteri et al., 2013) and their corrosion is the most important factor since it has a detrimental impact on the mechanical qualities and biocompatibility of the implant. As a result of corrosion and surface oxide film dissolution mechanisms additional ions are introduced into the body, and the excessive release of ions from an implant can lead to harmful biological reactions, consequently resulting in mechanical failure of the prothesis (Bidhendi & Pouranvari, 2012; Ferreira et al., 2003; Kumar et al., 2002; Manivasagam et al., 2010; Maradit et al., 2014; Pietak et al., 2008; Rivera et al., 2008; Uchi et al., 2001; Willert et al.,1996).

Due to their better biocompatibility and mechanical qualities similar to bone, titanium (Ti) and magnesium (Mg) alloy have recently become the most popular biomaterials for bone implantation in the human body (Burnat et al.,2013; Feng & Han, 2010; Okazaki, 2002; Leinenbach & Eifler, 2006; Poinern et al., 2012; Ravazi et al., 2010; Reifenrath et al., 2011; Shahba et al., 2011). Ti alloys mainly are a proper choice for implantation due to their excellent corrosion resistivity and bio-inertness due to the spontaneous formation of a 2 to 5 nm thick adhesive TiO_2 layer at the surface and the ability to become tightly integrated into bone (Estrada et al., 2019; Lim & Choe, 2019; Nasab et al., 2010). However, primarily due to fatigue failure, Ti-based implants such as artificial joints and bone plates are probably damaged (Okazaki & Gotoh, 2002; Topcu, 2020,). Dissolution of Ti^{+2} cations, wearing, and fretting causes corrosion pits which act as nucleation points for fatigue failure (Topcu et al., 2019’ Yilmaz et al., 2020). Thus, the fatigue strength of the material decreases (Barril et al., 2002; Komotori et al., 2007). Additionally, metal ions produced by corrosion and wear can cause inflammation, cell apoptosis, and other tissue-damaging effects (Biesiekierski et al., 2012; Wu et al., 2013).

Magnesium and its alloys, as opposed to Ti alloys, are highly bioactive and go through fast degradation in the body, rendering them excellent biomaterials in hard-tissue implants. Due to its matching mechanical and physical properties to cortial bone (Elastic Modulus: Mg: 40–45GPa, Cortical bone: 10–27GPa), stress shielding is prevented. It is also non-toxic, and the body's fourth most abundant cation, as well as the second most abundant intracellular cation. Furthermore, mg is essential for the metabolism at the cellular and enzymatic levels, and almost

50% of the ions are found in bones (Zeng et al., 2008; Zhang et al., 2009; Witte et al., 2008). Therefore, it is taken into the body daily and helps bone strength and development. However, due to their high bioactivity and low corrosion resistance in chloride-rich body fluids whose pH ranges from 7,4 to 7,6, they degrade fast and lose their mechanical integrity. The rapid acceleration of corrosion involves two fundamental problems. First, corrosion of Mg results in a crystalline film of magnesium hydroxide and hypodermic hydrogen gas bubbles that appear during the first week following surgery. Also, Mg particles might detach because of hydrogen stress corrosion, known as the chunk effect (Yun et al., 2009). The second problem is the loss of mechanical integrity between the implant and the surrounding bone tissue, which limits proper tissue regeneration (McCord, 1942; Wen et al., 2001). These drawbacks limit their application as a biomaterial. Hence, the corrosion properties and degradation of Mg-based alloys should be improved for biodegradable implant applications.

The biocompatibility of implants is strongly linked to physical and chemical features of its surface, such as its oxide composition, oxide thickness, surface roughness, and surface free energy. Based on the current project's goal, anodization has the best probability of meeting these requirements. It is an electrolytic oxidation process in which a metal anode is turned into an oxide layer with corrosion-protective and functional qualities. This method can improve coating thickness, hardness, corrosion, and wear resistance while also improving primer adhesion over bare metal. Anodization with a desirable outcome can be achieved upon the careful design of several parameters, such as electrolyte composition (De Oliveria & Antunes, 2018; Hsiao & Tsai, 2005; Ono et al., 2004; Park et al., 2008; Zaffora et al., 2021), anodizing parameters such as current density and voltage (De Oliveria & Antunes, 2018; Li et al., 2008; Mizutani et al., 2003; Ono et al., 2004; Bandeira et al., 2020), substrate effects including purity, the concentration of alloying elements (Hiromoto et al., 2008; Khaselev & Yahalom,1998; Mizutani et al., 2003), doping elements (Wang et al., 2020; Chatterjee et al., 2022) and substrate type. The applied voltage or current is powerfully influential in the anodizing behavior of the metal. Different passive and active states can be identified based on the applied voltage/current, substrate, and electrolyte (Yerokhin et al., 1999).

According to the Food and Drug Administration, the number of individuals suffering from implants climbed from around 2.500 to more than 5.000 between 2010 and 2011 (Warranty, 2016). Determining a solution to this problem has become necessary to increase the implant product's lifespan by improving its corrosion resistivity. A number of potential techniques for improving the corrosion resistance of implantation material are both expensive and time-consuming. As a result, the goal of this research is to develop a simple and cost-effective anodization method for implanting materials for a particular period of time and studying their corrosion behavior. In the current study, two different alloys, e.g., Ti-alloys (Ti6Al4V) and Mg-alloys (MgAZ31B), were selected to study the corrosion behavior. The corrosion penetration rates of these alloys were determined periodically by performing electrochemical analysis in 3 different electrolytic mediums (deionized (DI) water, 3% sodium chloride (NaCl) solution and phosphate-buffered saline (PBS) solution (1x)) for different periods. The results showed that the anodization process decreases the corrosion rate, and the study provided specific information on the lifespan of the implant in the human body.

The novelty of this study includes the following: (1) for the first time, anodized metallic biomaterials were prepared using phosphoric acid and oxalic acid solutions at different levels, and (2) electrochemical behavior of those biomaterials was investigated for the improved corrosion resistance. This approach has many advantages over other approaches in improving the corrosion resistance for the body conditions. Furthermore, the essential information from the present work can also be used to address other related biomaterials corrosion and degradation issues for different tissue engineering and scaffolding applications.

2. EXPERIMENT

2.1. Materials and Anodization Process

Electrolyte passivation or anodizing was performed on Ti6Al4V and MgAZ31B alloys in different electrolyte solutions. For anodization, the samples were cut from a plate sample. The dimensions of the samples were 100 mm x 35 mm x 1 mm for Mg alloy and 55 mm x 30 mm x 5 mm for Ti alloy. First, using soap and DI water, all samples' surfaces were smoothed, cleaned. Later on, they were dried to clear out debris and carbon precipitation. Then, the electrolyte solution was transferred to the anodization pot where the anodization process would be held. The anode from the voltage supply end was then linked to the sample, with the cathode connected to the electrolyte solution. For Ti6Al4V, the anodization was performed in 0,5 M oxalic acid and 0,4 M phosphoric acid for 60 seconds and 45 seconds. For MgAZ31B, the anodization was performed in 1 N potassium hydroxide (KOH) and 0,4 M phosphoric acid solution for 15min and 4 min. In both instances, the applied voltage (20V) was retained the same. The specimens were removed from the electrolyte solution after anodization and dried appropriately to improve the color, implying the ground oxide layer. Later, specimens were adequately cleaned and dried again for a more extended period to support the surface layer. The same anodization procedure was pursued in all specimens.

2.2. Electrochemical Analysis

Electrochemical study of the corrosion rate for both anodized and non-anodized Ti and Mg alloy test samples were submerged in 3% NaCl solution, PBS solution (1x), and DI water for different time. A 3% NaCl solution (0,5 M) was formulated by dissolving 29,22 g of NaCl crystal salt in 1,000 ml of DI water. 1X PBS solution was prepared by diluting10X PBS. During the preparation of the PBS solution, the pH was kept in the range of 7,5–7,7, which is the usual pH of the human body. Deionized water was used for the experiments being another immersion environement. For all test samples, Tafel and Nyquist's curves are collected in three different solutions using Gamry corrosion cell and the Gamry reference 600 potentiostat. For the Ti alloy samples, the corrosion rate data were collected every five days in each solution. For the Mg alloy samples, the data were collected on an hourly basis in each solution. In order to obtain accurate corrosion rate data, three to five repeated tests were conducted, and the average value was used to represent each data set. Corrosion rates were investigated after 1.080 hours of immersion for Ti alloy and until pitting started for Mg alloy.

2.3. Optical Microscopy

The surface appearance of the test samples was observed from microscope images of 10x and 20x magnification using a computer-integrated optical microscope (Zeiss Axio Imager). The images were taken before and after the anodization process for all samples periodically.

3. RESULTS AND DISCUSSION

3.1. Anodization of Metallic Implants

The corrosion rate of the metal used for the biomaterial in different corrosive media can be utilized to determine the lifetime expectancy of the biomaterial. This is because the body's internal environment is well buffered and preserved at a pH of around 7,4 at 37°C. Essentially, the harshness of this environment is controlled by two factors. First, as an electrolyte, saline solution promotes corrosion and hydrolysis electrochemical reactions. Second, many cellular and molecular species in tissues are capable of catalyzing specific chemical reactions or destroying some foreign components. Metals used in the human body should have a strong resistance to corrosion in order to have a longer life period. (Uchi et al., 2001).

Anodization is one way of enhancing the corrosion resistivity of a material (Karambakhsh et al., 2012; Nishinaka et al., 2018) in which The metal is submerged in an electrolyte bath, and a circuit is used to conduct the current. While the metal works as an anode, the cathode electrode is put inside the anodizing tank. As the cathode increases the release of oxygen atoms from the electrolyte solution, the anode creates a metal oxide layer. The anodized surface layer thickness varies from a few nm to several μm (Ahmad, 2006; Revie, 2008). Anodization produces metal oxide deposits on a material's surface, thus eliminating more chemical reactions through an electrolytic passivation process (Park et al., 2007). Depending on the material properties being anodized, it could be acidic or basic anodization (Narayanan & Seshadri, 2007). In acid electrolytes such as oxalic acid, sulfuric acid, and phosphoric acid, the rate of anodic film generation is substantially faster than the rate of dissolution for Ti6Al4V. The rate of anodic film generation for MgAZ31B, however, varies with the acid and base solutions, such as phosphoric acid (PhoA) and potassium hydroxide (KOH) solution (Fattah & Joni, 2015; Sul et al., 2001). The bare metal surface is layered with an anodic oxide surface that is corrosion-resistive, decorative, hard, and durable.

Images of anodized Ti6Al4V and MgAZ31B are given in Figure 1. Figures 1B and 1C show a change in surface color of Ti6Al4V following anodization with both phosphoric acid and oxalic acid using a 20V DC current. A smooth surface layer formed on the bare Ti alloy after the anodization. Figures 1D to 1F show anodized and non-anodized MgAZ31B samples. As a result of anodization, the surfaces of the anodized samples are seen to be dark ash color.

The anodization process can be affected by several parameters such as acid concentration, the bath's temperature, additives, current density, reaction time, applied voltage, efficient bath agitation, bath cooling, etc. (Callister & Rethwisch, 2007). In the current work, the anodization process was completed for a different period depending on the materials and the electrolyte solutions. The applied voltage of 20V was held constant in both cases to achieve a similar comparison between the materials in the same setting so that the color could not differ from sample to sample. Even though the anodization layer's thickness changes depending on several parameters, the tests' primary concern was investigating the anodization of the different materials exposed to the same voltage. If stability and consistency can be maintained during the anodization, this process is stable and trustworthy. Otherwise, performing anodization on a single sample would necessitate numerous trials.

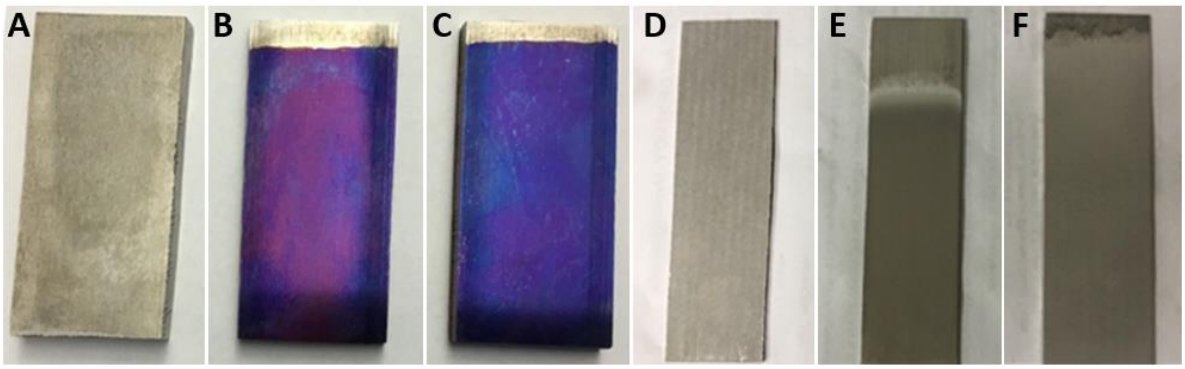

Figure 1. Images of Bare and Anodized Ti and Mg Alloys, (A) Bare Ti6Al4V, (B) Ti6Al4V After Anodization in Phosphoric Acid, (C) Ti6Al4V After Anodization in Oxalic Acid, (D) Bare MgAZ31B, (E) MgAZ31B After Anodization in Phosphoric Acid, (F) MgAZ31B After Anodization in Potassium Hydroxide

3.2. Optical Microscope Images

The difference in grain boundary with and without anodization was captured using optical microscopy pictures. Due to the anodization process, colored layers were formed on the surfaces. The colored surface layers in the microscopic images became more prominent with the increased drying time. The boundary grain of Ti6Al4V was seen with a magnification of 10x and 20x for both anodized and non-anodized samples, as shown in the magnified optical microscopic photographs in Figure 2. Both phosphoric acid and oxalic acid anodization are indicated by a distinct layer of bluish-purple tint.

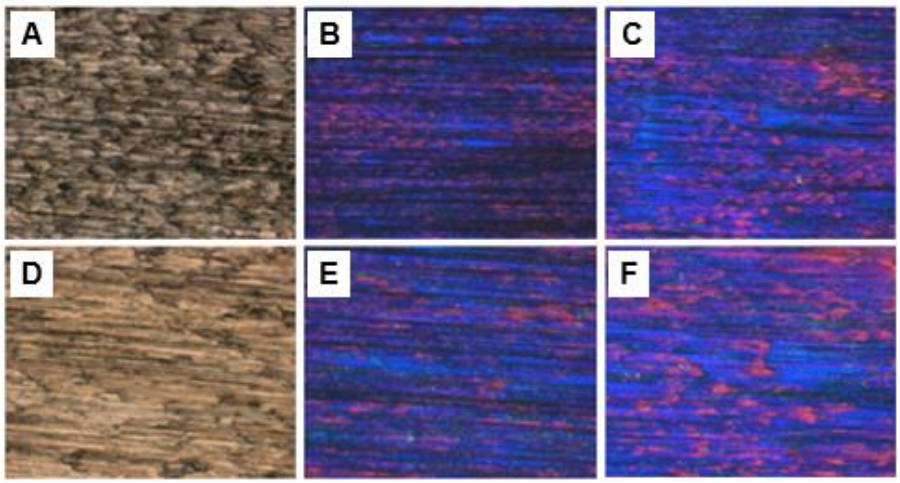

Figure 2. Optical Microscopic Images for Anodized and Non-Anodized Ti6Al4V, (A) Before Anodization (10x), (B) After Anodization in Phosphoric Acid (10x), (C) After Anodization in Oxalic Acid (10x), (D) Before Anodization (20x), (E) After Anodization in Phosphoric Acid (20x), (F) After Anodization in Oxalic Acid (20x)

Figure 3 shows the boundary grain magnified optical microscopic images for MgAZ31B, with magnifications of 10x and 20x for both anodized and non-anodized samples. For potassium hydroxide and phosphoric acid solutions, however, a distinct layer was seen. When anodizing with KOH, the surface smoothness was better, whereas when anodizing in phosphoric acid solution, the smoothness was less.

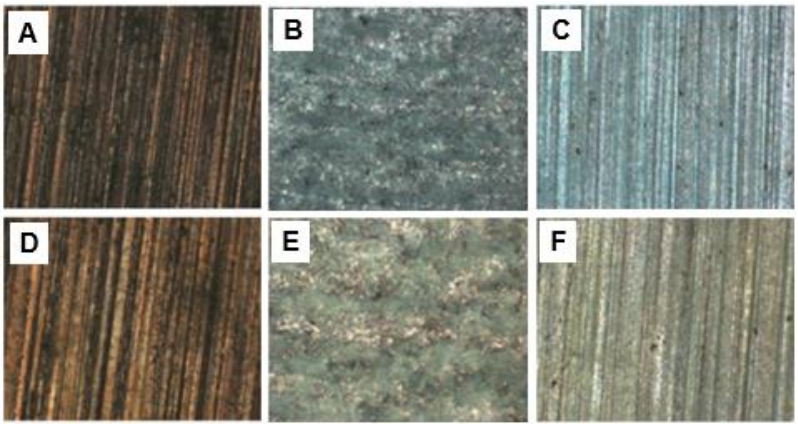

Figure 3. Optical Microscopic Images for Non-Anodized and Anodized MgAZ31B, (A) Before Anodization (10x), (B) After Anodization in Phosphoric Acid (10x), (C) After Anodization in Potassium Hydroxide (10x), (D) Before Anodization (20x), (E) After Anodization in Phosphoric Acid (20x), (F) After Anodization in Potassium Hydroxide (20x)

3.3. Electrochemical Analysis of Corrosion Measurement

Corrosion is the disintegration of metals due to numerous environmental factors to become more chemically stable. It is simply a surface reaction propagating vigorously progressively by affecting the material`s integrity. Corrosion causes localized material loss in the presence of a water or salt solution (Schutze, 2000). This electrochemical reaction takes place at the surface and involves the exchange of charges or ions across the solid-liquid interface. Simultaneously, two types of electrochemical reactions occur: the first is an anodic reaction, in which the metal is ionized and a cation forms, which is then hydrolyzed in solution, and the second is a cathodic reaction, in which the produced electrons from the anodic reaction are consumed in the reduction of protons in hydrogen or the reduction of oxygen in water (Marcus, 2011).

Corrosion is a mixed electrode process that operates at a mixed potential or corrosion potential, which is determined by comparing the potential differences between corroding and stable electrodes. This potential can also be utilized to assess the composition of corrosion products and to predict environmental changes that may impede the corrosion attack. In this research, the corrosion rate was calculated from the kinetics of the electrochemical corrosion process. Assume that activation regulates cathodic and anodic reactions on an electrode surface. The corrosion potential is not close enough to the individual cathodic and anodic reaction equilibrium potentials. In that scenario, equations (1) and (2) can be used to calculate the corrosion-reaction kinetics and electrode potential of any reversible half-cell reaction. (Jones, 1996):

$$E = E° + \frac{RT}{nF} ln \frac{[\mathrm{Ox}]}{[\mathrm{Red}]} \tag{1}$$

$$i = i_{corr} \left[\exp\left(\frac{\alpha n F}{RT}\eta\right) - \exp\left(\frac{-\beta n' F}{RT}\eta\right)\right] \tag{2}$$

where i the measured current density, i_{corr} is the corrosion current density, F is Faraday's constant, R is the universal gas constant, T is the absolute temperature, and n and n' are the number of electrons transferred in the anodic and cathodic reactions respectively, α and β are coefficients related to the potential drop, and η is the over-potential. When there is a sufficiently large value of applied potential, equation (2) can be simplified to equations (3) to (4) (Jones, 1996; Tan & Revie, 2012). For anodic polarization, when $\eta >> RT/\beta n'F$,

$$i = i_{corr}\left[\exp\left(\frac{\alpha nF}{RT}\eta\right)\right] \quad (3)$$

where

$$\eta = -\frac{2.3RT}{\alpha F}\log i_{corr} + \frac{2.3RT}{\alpha F}\log i$$

Similarly, for cathodic polarization, when $-\eta >> RT/\alpha nF$,

$$i = i_{corr}\left[\exp\left(\frac{-\beta n'F}{RT}\eta\right)\right] \quad (4)$$

where

$$-\eta = -\frac{2.3RT}{\alpha F}\log i_{corr} + \frac{2,3RT}{\alpha F}\log i$$

Hereafter, from equations (3) and (4), the Tafel equation can be obtained as

$$|\eta| = a + b\log i \quad (5)$$

where a and b are the anodic and cathodic polarization constants respectively (Jones, 1996; Tan & Revie, 2012).

In the electrochemical study, all of the samples were evaluated to attain both the Tafel and Nyquist curves for all three solutions. Depending on the Tafel equation and the corrosion rate calculation formula, the corrosion parameters and rate are both provided by Tafel curves. For both anodized and non-anodized Ti and Mg alloys, the experiments were carried out to assess how the corrosion rate changed over time at various intervals. When soaking the samples in various solutions on a regular basis, Nyquist curves revealed the corrosion patterns. The Tafel curve extrapolation method is described in Equation (5). Based on this method, the value of either the cathodic or the anodic current at the intersection is i_{corr}. Extrapolating the linear parts of the Tafel plot back to their intersection, where the over-potential should be zero, is the best technique to measure the corrosion current icorr (Ahmad, 2006; Revie, 2008). Figure 4 shows how to extract corrosion parameters from the Tafel plot, such as corrosion current, icorr, and corrosion potential, Ecorr. This is one of the most accurate methods for determining a metal's corrosion parameter (Ahmad, 2006). After obtaining the corrosion current or corrosion current density, icorr, the following formulas are used to assess the level of corrosion penetration (Ahmad, 2006):

$$CPR(\mu m/y) = \frac{3{,}27\ \mathrm{M}\ i_{corr}}{n\rho}$$

$$CPR(mpy) = \frac{0{,}129\ \mathrm{M}\ i_{corr}}{n\rho}$$

$$WL(mg/cm^2y) = \frac{0{,}327\ \mathrm{M}\ i_{corr}}{n}$$

Where CPR is corrosion penetration rate, MPY is mili-inch per year, WL is weight loss, i_{corr} is the current density (mA/m^2), M is the atomic weight (g/mol), ρ is density (g/cm^3), and n is valence of the metal ion (Ahmad, 2006).

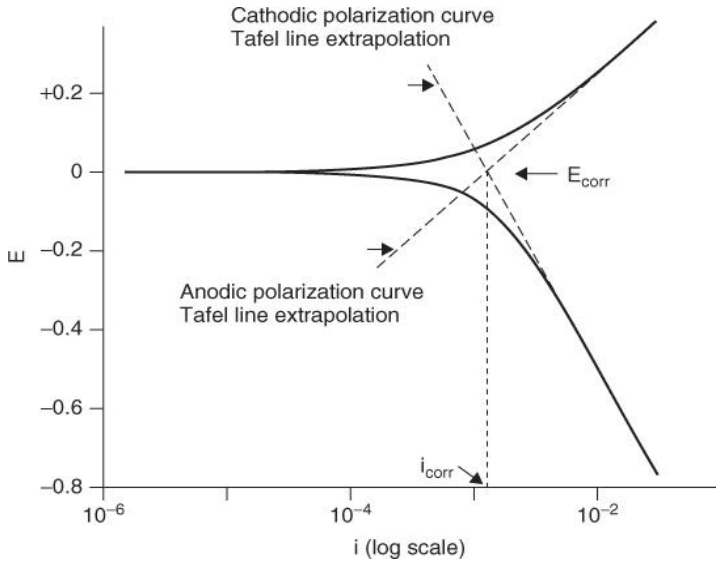

Figure 4. Tafel Curve Extrapolation for Determining Electrochemical Corrosion Parameters (Revie, 2008)

Day-wise, Tafel curves to measure the corrosion behavior of all samples immersed in three different solutions for various periods are plotted. The same equivalent weights and densities were used for the corrosion rate calculation for all samples. From Tafel curves, the corrosion parameters were obtained, and at the same time, Nyquist curves of the corresponding samples were also plotted to further show the same corrosion pattern of the respective samples. A few examples of Tafel and Nyquist plots belonging to Ti6Al4V and MgAZ31B to calculate the corrosion rate are given in Figure 5.

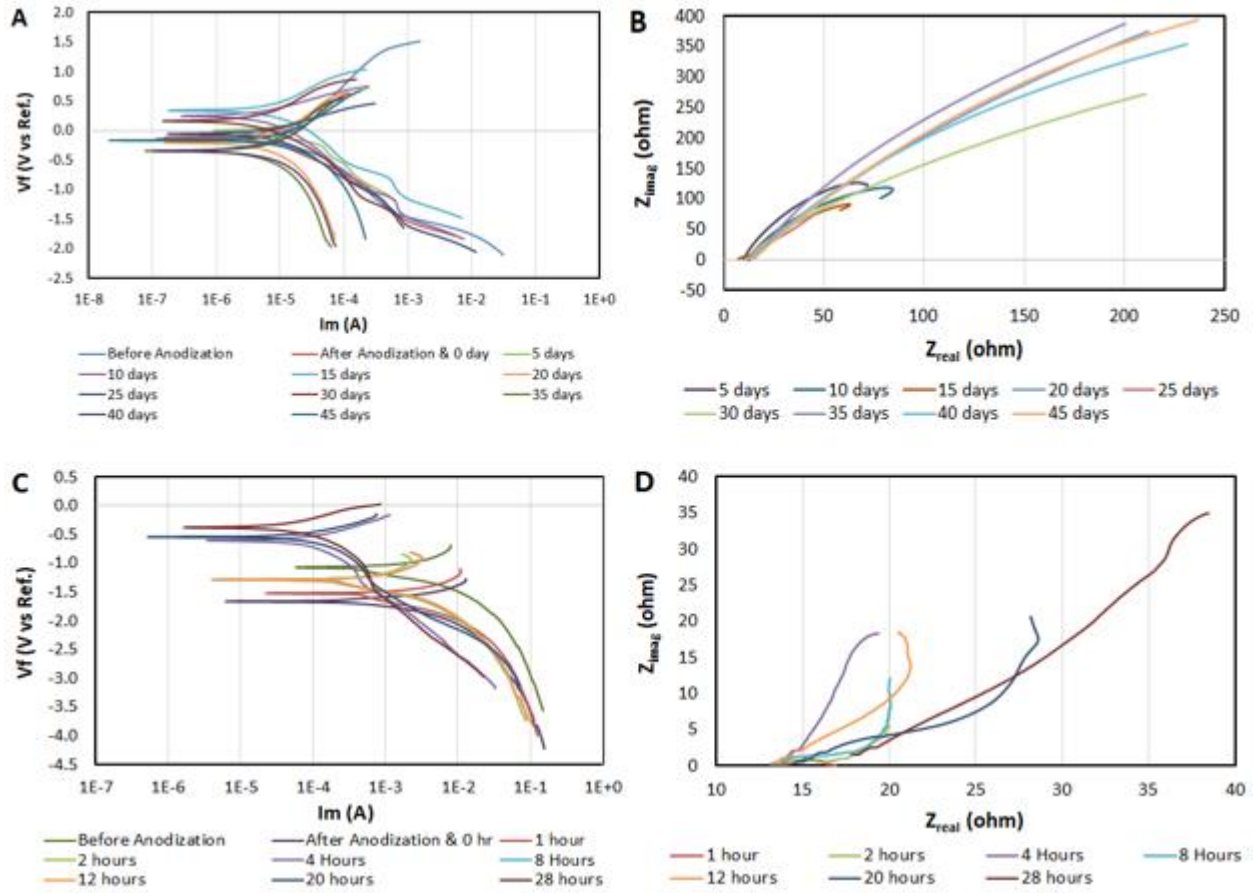

Figure 5. Tafel and Nyquist Plots of Ti6Al4V and MgAZ31B alloys A) Tafel Curves of Anodized (in 0.4 M Phosphoric Acid) Ti6Al4V Immersing in 3% NaCl Solution, B) Nyquist Plots of Anodized (in 0,4 M phosphoric acid) Ti6Al4V Immersing in 3% NaCl Solution, C) Tafel Curves of Anodized (in 0.4 M Phosphoric Acid) MgAZ31B Immersing in 3% NaCl Solution, D) Nyquist Plots of Anodized (in 0,4 M Phosphoric Acid) MgAZ31B Immersing in 3% NaCl Solution

3.4. Corrosion Measurement of Anodized and Non-anodized Ti6Al4V

Electrochemical corrosion tests on anodized and non-anodized Ti-alloy samples immersed in three distinct solutions for gradually longer time periods were carried out on a regular basis. PBS with a pH of 7,4–7,7 was utilized to simulate the typical body condition, whereas 3 percent NaCl solution and DI water were used to reflect the highest and lowest corrosion conditions, respectively. To investigate the relationship between the mentioned variables and the improvement in corrosion resistivity of anodized samples, the primary focus was on establishing and comparing the corrosion behaviors of anodized and non-anodized specimens. This is a simple and reliable method for determining corrosion behavior as well as the rate of corrosion of a material in various solutions in order to determine the life expectancy of biomaterials.

Figure 6A demonstrates the corrosion behavior in the NaCl solution as a function of immersion time. As can be seen, the corrosion rate of both anodized and non-anodized Ti alloys rose with immersion time; however, the rise in non-anodized samples is much greater than the increase in anodized samples with the same immersion time. The corrosion rate for both anodized and non-anodized samples dropped after anodization and rose with increasing immersion duration, eventually stabilizing after 15–20 days for both anodized and non-anodized samples. Furthermore, the corrosion rate of the anodized samples did not grow as much as the corrosion

rate of the non-anodized samples following immersion in the NaCl solution, implying that the anodized sample has superior corrosion resistance than the non-anodized sample.

The corrosion behavior of anodized and non-anodized Ti6Al4V immersed in PBS and DI water, respectively, is shown in Figures 6B and 6C. When corrosion rates for anodized and non-anodized Ti alloys are compared with immersion time in PBS solution, it is discovered that following anodization, the corrosion rate initially decreases and then increases with immersion duration for all samples. However, as compared to the non-anodized sample, which has superior corrosion resistance than the raw Ti6Al4V alloy, the incremental rate for anodized samples is low. After ten days of immersion, the corrosion rate stabilizes. The difference between the corrosion rates of the non-anodized and anodized samples, on the other hand, widens over time, showing that the anodized sample has a reduced corrosion rate.

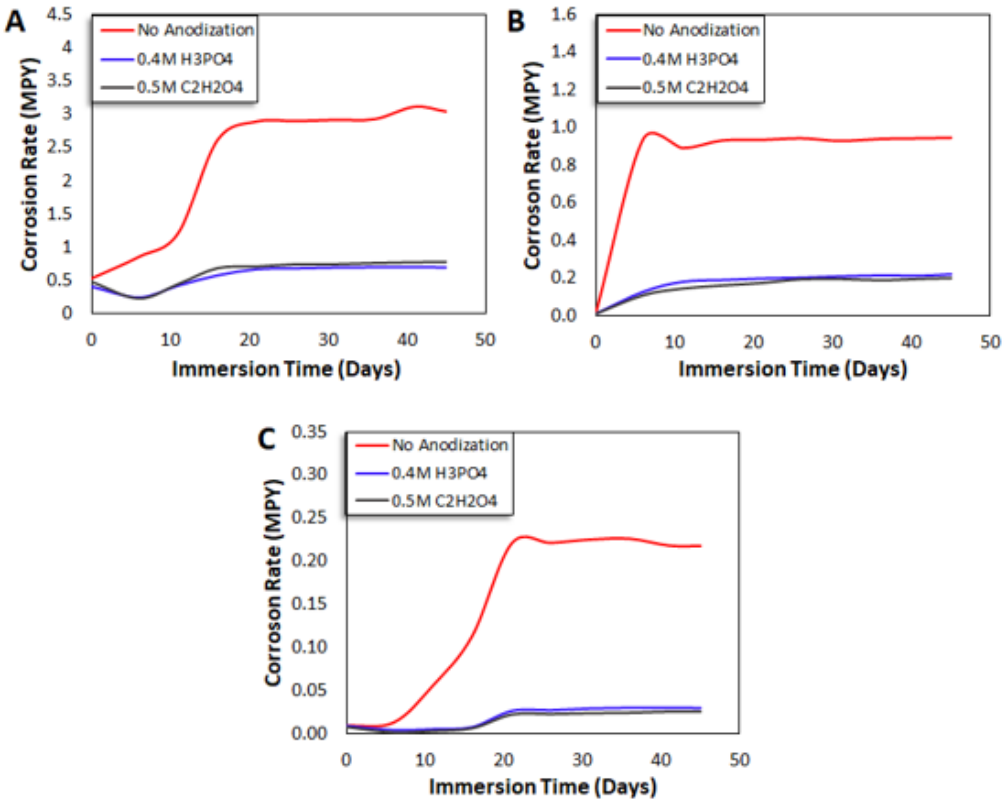

Figure 6. Corrosion Rate of Ti6Al4V Immersed in A) 3% NaCl Solution, B) PBS Solution (1x), and C) DI Water

Figure 7 demonstrates the comparison of corrosion rates of all anodized and non-anodized Ti-alloys. In our study, the peak value of the corrosion rate was chosen to compare the corrosion rate among all the samplesIn NaCl solution, bare Ti-alloy samples corrode faster than in PBS solution or DI water. This is an expected scenario of the sodium ions in a salt solution which creates a rigorous corrosion environment. The corrosion rate in NaCl solution reaches 3,1 mpy, which is extremely high when compared to PBS and DI water, which have corrosion rates of roughly 0,9 mpy and 0,2 mpy, respectively. The anodization procedure also increases the corrosion resistance of the Ti-alloy, according to the findings. For varied immersion times, the maximum corrosion rate of Ti6Al4V anodized in 0,5 M oxalic acid is lower than that of 0,4 M phosphoric acid, and even lower in PBS and DI water than in NaCl solution. As a result, it can be stated that anodization has a favorable impact on Ti alloy corrosion resistance, with anodization in oxalic acid having the highest corrosion resistance of all the samples.

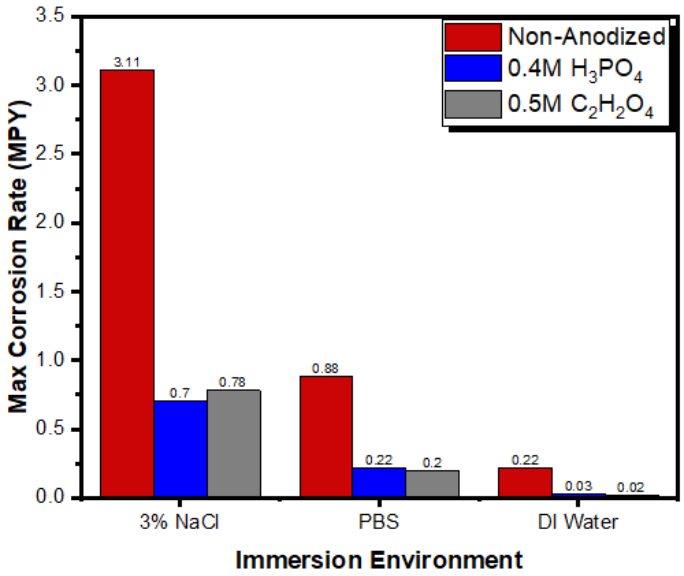

Figure 7. Corrosion Behavior Comparison of Anodized and Non-Anodized Ti6Al4V Immersed in Various Solutions

3.5. Corrosion Measurement of Anodized and Non-anodized MgAZ31B

Corrosion behavior and comparison between non-anodized and anodized MgAZ31B were represented respectively in Figures 8 and 9. In all conditions, the corrosion rate of bare Mg-alloy in NaCl and PBS solutions is higher than in DI water, as shown. Among the NaCl and PBS solutions, NaCl has a greater negative impact on bare Mg-alloy corrosion and pitting (Figure 9). The corrosion and pitting effects of a 3 percent NaCl solution are greater than those of PBS and DI water; nevertheless, due to the anodization process, the maximum corrosion rate is lower than that of non-anodized samples in all circumstances.

The corrosion rate of Mg-alloy samples drops after the anodization process, then climbs and remains constant with immersion time in a 3 percent NaCl solution (Figure 8A). For the non-anodized sample, however, the corrosion rate increases rapidly and then stabilizes after a period of time. A similar trend was also observed in PBS and DI water solution (Figures 8B and 7C)., Corrosion rate drops significantly between 12 to 20 hours of the immersion due to pitting propagation, as it creates holes on the sample surface area by reducing chemical affinity and damaging oxide layer from the surface of the material. In DI water (Figure 8C), the corrosion rate was the lowest before immersion as compared to NaCl or PBS solutions and increased slowly with immersion time. Corrosion currents and voltages were nearly constant, with just small variations.

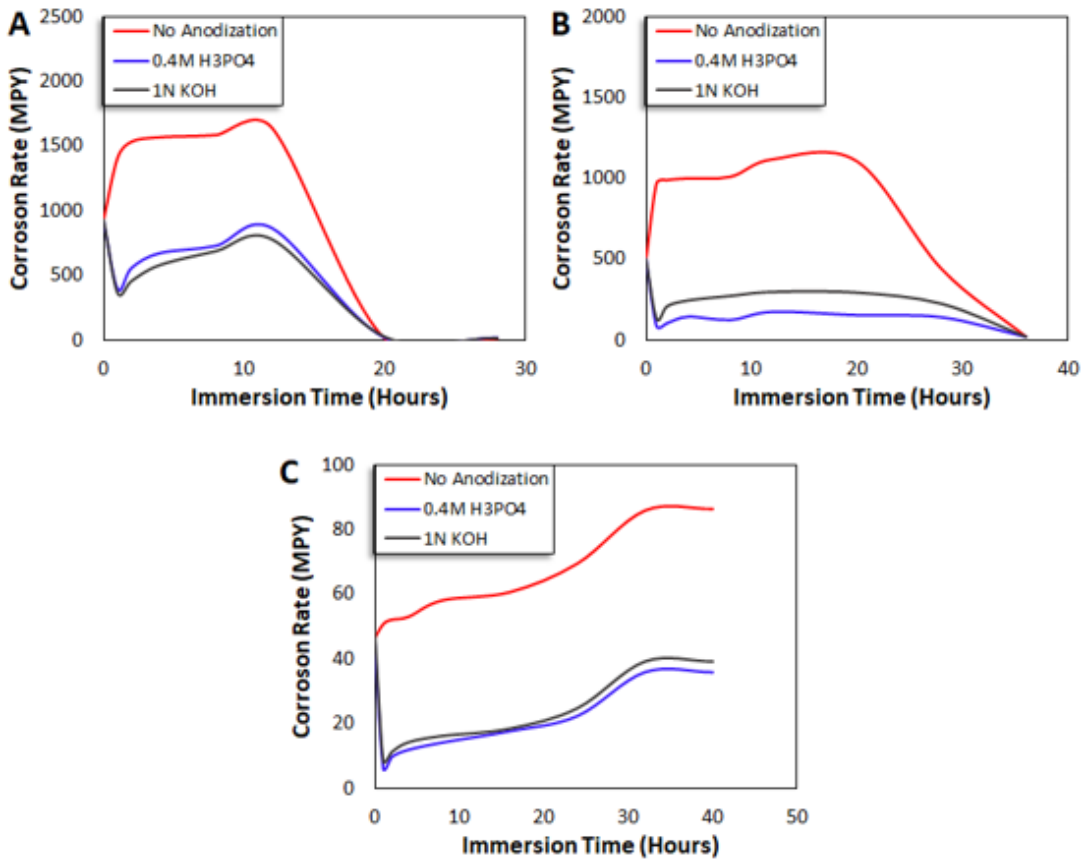

Figure 8. Corrosion Rate of MgAZ31B Immersed in
A) 3% NaCl Solution, B) PBS Solution (1x), and C) DI Water

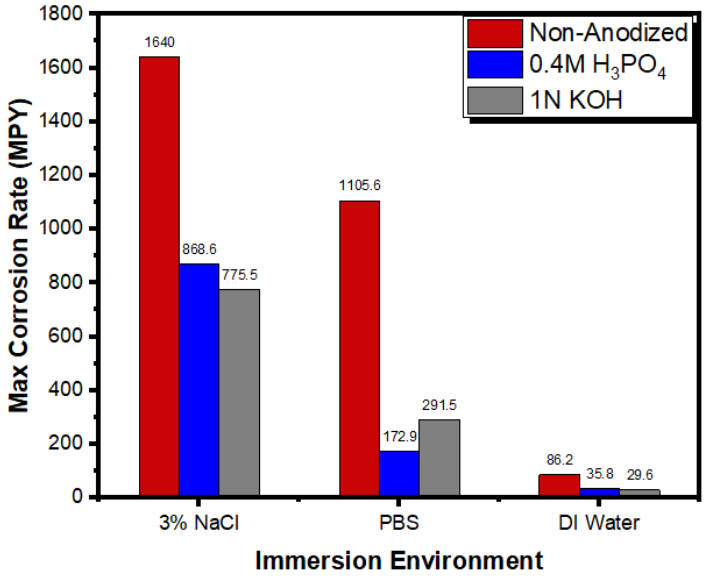

Figure 9. Corrosion Behavior Comparison of Anodized and
Non-Anodized MgAZ31B Immersed in Various Solutions

Ti-alloys, on the other hand, were observed to be far more corrosion resistant than Mg-alloys. In NaCl solution, the maximum corrosion rates for anodized Ti6Al4V and MgAZ31B were 0,78447 and 868,63 mpy, respectively. In the same NaCl solution for the same duration of immersion time, the maximum rates of corrosion for non-anodized Ti6Al4V and MgAZ31B were 3,0430 mpy and 1640,02 mpy, respectively. Overall, anodization enhanced the corrosion resistance of

both alloys significantly. This electrochemical modeling approach for corrosion determination might save a time and money. Our findings on the anodization process could help metallic implants and stents last longer.

4. CONCLUSIONS

This study looked at the corrosion characteristics of anodized and non-anodized metallic biomaterial alloys. To compare the lifetimes of the biomaterials samples were immersed in NaCl, PBS, and DI water solutions for varying amounts of time. As a result of the anodization process in various acidic and basic electrolyte solutions, a natural oxide layer formed on the surfaces of biomaterial alloy samples, increasing their corrosion resistance. Pitting is thought to be the cause of corrosion in Mg alloys, which began after about 15–20 hours in the NaCl solution. Furthermore, the corrosion rate of anodized samples did not grow as much as that of non-anodized samples before immersion during prolonged immersion periods. Anodization generates a smooth surface layer on the biomaterial, which minimizes the corrosion rate, according to optical microscopic images. Therefore, it can be established that even in more corrosive mediums, surface modification using anodization improved the corrosion resistance of the biomaterial alloys and increased the lifetime of the metallic biomaterial implant alloys. Our corrosion behavior research could provide unique insight into the biomaterial implants' long-term durability, rather than just a few months. In the future, post-anodizing annealing can be used to demonstrate the influence of thermal treatment on microstructure and, as a result, corrosion resistance. Cytotoxicity studies should also be carried out to determine the biocompatibility and endurance of the oxidized layers in the human body environment.

Contribution of The Authors
All authors contributed equally to this work.

Acknowledgment
The authors greatly acknowledge Wichita State University for its financial and technical support of this study.

Statement of Interest Conflict
There is no interest confliction between the authors.

Data Availability
The raw/processed data required to reproduce these findings cannot be shared at this time as the data also forms part of an ongoing study.

Statement of Research and Publication Ethics
Research and publication ethics were observed in the study.

REFERENCES

Ahmad, Z. (2006). Principles of corrosion engineering and corrosion control. *Elsevier*.

Bandeira, R. M., Rêgo, G. C., Picone, C. A., van Drunen, J., Correr, W. R., et al. (2020). Alternating current oxidation of Ti–6Al–4V alloy in oxalic acid for corrosion-resistant surface finishing. *SN Applied Sciences*, 2(6), 1-14.

Barril, S., Debaud, N., Mischler, S. & Landolt, D. (2002). A tribo-electrochemical apparatus for in vitro investigation of fretting–corrosion of metallic implant materials. Wear, 252(9-10), 744-754.

Bidhendi, H.R.A. & Pouranvari, M. (2012). Corrosion study of metallic biomaterials in simulated body fluid. *Metallurgical and Materials Engineering*, 17(1), 13-22.

Biesiekierski, A. Wang, J., Gepreel, M. A. H., & Wen, C. (2012). A new look at biomedical Ti-based shape memory alloys. *Acta Biomaterialia*, 8(5), 1661-1669.

Burnat, B. Walkowiak-Przybyło, M., Błaszczyk, T., & Klimek, L. (2013). Corrosion behaviour of polished and sandblasted titanium alloys in PBS solution. *Acta of Bioengineering and Biomechanics*, 15(1), 87-95.

Callister, W. D. & Rethwisch, D. G. (2007). Materials science and engineering: an introduction 7, 665-715. *John Wiley & Sons*, New York.

Chatterjee, S. (2022). Titanate incorporated anodized coating on magnesium alloy for corrosion protection, antibacterial responses and osteogenic enhancement. *Journal of Magnesium and Alloys*, 10(4), 1109-1123.

De Oliveira, L.A. & Antunes, R. A. (2018). Influence of the electrolyte composition on the corrosion behavior of anodized AZ31B magnesium alloy. *Metals - Open Access Metallurgy Journal*, 11(10), 1573.

De Viteri, V.S. & Fuentes, E. (2013). Titanium and titanium alloys as biomaterials. *Tribology-fundamentals and advancements*, *5*, 154-181.

Estrada-Cabrera, E., Torres-Ferrer, L. R., Aztatzi-Aguilar, O. G., De Vizcaya-Ruiz, A., Meraz-Rios, M. A., et al. (2019). Chitosan-bioglass coatings on partially nanostructured anodized Ti-6Al-4V alloy for biomedical applications. *Surface and Coatings Technology*, *375*, 468-476.

Fattah-Alhosseini, A. & Joni, M. S. (2015). Effect of KOH Concentration on the Microstructure and Electrochemical Properties of MAO-Coated Mg Alloy AZ31B. *Journal of Materials Engineering and Performance*, 24(9), 3444-3452.

Feng, A. & Han, Y. (2010). The microstructure, mechanical and corrosion properties of calcium polyphosphate reinforced ZK60A magnesium alloy composites. *Journal of Alloys and Compounds*, 504(2), 585-593.

Ferreira, M. E., de Lourdes Pereira, M., e Costa, F. G., Sousa, J. P. & de Carvalho, G.S. (2003). Comparative study of metallic biomaterials toxicity: A histochemical and immunohistochemical demonstration in mouse spleen. *Journal of Trace Elements in Medicine and Biology*, 17(1), 45-49.

Hermawan, H., Ramdan, D. & Djuansjah, J.R. (2011). Metals for biomedical applications. *Biomedical engineering-from theory to applications*, 1, 411-430.

Hiromoto, S., Shishido, T., Yamamoto, A., Maruyama, N., Somekawa, H. & Mukai, T. (2008). Precipitation control of calcium phosphate on pure magnesium by anodization. *Corrosion Science*, 50(10), 2906-2913.

Hsiao, H.Y. & Tsai, W.T. (2005). Characterization of anodic films formed on AZ91D magnesium alloy. *Surface and Coatings Technology*, 190(2-3), 299-308.

Jones, D.A. (1996). Principles and prevention of corrosion prentice hall. *Saddle River*. New Jorsey.

Karambakhsh, A., Afshar, A. & Malekinejad, P. (2012). Corrosion resistance and color properties of anodized Ti-6Al-4V. *Journal of Materials Engineering and Performance*, 21(1), 121-127.

Khaselev, O. & Yahalom, J. (1998). The anodic behavior of binary Mg-Al alloys in KOH-aluminate solutions. *Corrosion Science*, 40(7), 1149-1160.

Komotori, J., Hisamori, N. & Ohmori, Y. (2007). The corrosion/wear mechanisms of Ti–6Al–4V alloy for different scratching rates. *Wear*, 263(1-6), 412-418.

Kumar, N., Langer, R. S. & Domb, A. J. (2002). Polyanhydrides: an overview. *Advanced Drug Delivery Reviews*, 54(7), 889-910.

Leinenbach, C. & Eifler, D. (2006). Fatigue and cyclic deformation behaviour of surface-modified titanium alloys in simulated physiological media. *Biomaterials*, 27(8), 1200-1208.

Li, L. L., Cheng, Y. L., Wang, H. M. & Zhang, Z. (2008). Anodization of AZ91 magnesium alloy in alkaline solution containing silicate and corrosion properties of anodized films. *Transactions of Nonferrous Metals Society of China*, 18(3), 722-727.

Lim, S.G. & Choe, H. C. (2019). Bioactive apatite formation on PEO-treated Ti-6Al-4V alloy after 3rd anodic titanium oxidation. *Applied Surface Science*, 484, 365-373.

Maradit-Kremers, H., Crowson, C. S., Larson, D., Jiranek, W. A. & Berry, D.J. (2014). Prevalence of total hip (THA) and total knee (TKA) arthroplasty in the United States. *In Abstract presented at: AAOS Annual Meeting*.

Manivasagam, G., Dhinasekaran, D. & Rajamanickam, A. (2010). Biomedical implants: corrosion and its prevention-a review. *Recent Patents on Corrosion Science.* 2, 40-54

McCord, C. P. (1942). Chemical gas gangrene from metallic magnesium. *Indust Med*, 11, 71-78.

Mizutani, Y., Kim, S. J., Ichino, R. & Okido, M. (2003). Anodizing of Mg alloys in alkaline solutions. *Surface and Coatings Technology*, 169, 143-146.

Marcus, P. (Ed.). (2011). Corrosion mechanisms in theory and practice. *CRC press*. Florida.

Nasab, M. B., Hassan, M. R. & Sahari, B. B. (2010). Metallic biomaterials of knee and hip-a review. *Trends Biomater. Artif. Organs*, 24(1), 69-82.

Narayanan, R. & Seshadri, S. K. (2007). Phosphoric acid anodization of Ti–6Al–4V–Structural and corrosion aspects. *Corrosion Science*, 49(2), 542-558.

Nishinaka, K., Salman, S. A., Kuroda, K. & Okido, M. (2018). Characterization and Structure Analysis of the Anodic Film Formed on AZ31 Mg Alloy in KOH Alkaline Solution with Various Additives. In *Key Engineering Materials*, 786, 159-164.

Okazaki, Y. (2002). Effect of friction on anodic polarization properties of metallic biomaterials. *Biomaterials*, 23(9), 2071-2077.

Okazaki, Y. & Gotoh, E. (2002). Implant applications of highly corrosion-resistant Ti-15Zr-4Nb-4Ta alloy. *Materials Transactions*, 43(12), 2943-2948.

Ono, S., Miyake, M. & Asoh, H. (2004). Effects of formation voltage and electrolyte ions concentration on the structure and passivity of anodic films on magnesium. *Journal of Japan Institute of Light Metals*, 54(11), 544-550.

Park, I. S., Jang, Y. S., Kim, Y. K., Lee, M. H., Yoon, J. M. & Bae, T. S. (2008). Surface characteristics of AZ91D alloy anodized with various conditions. *Surface and Interface Analysis: An International Journal devoted to the development and application of techniques for the analysis of Surfaces, Interfaces and Thin Films*, 40(9), 1270-1277.

Park, Y. J., Shin, K. H. & Song, H. J. (2007). Effects of anodizing conditions on bond strength of anodically oxidized film to titanium substrate. *Applied Surface Science*, 253(14), 6013-6018.

Pietak, A., Mahoney, P., Dias, G. J. & Staiger, M. P. (2008). Bone-like matrix formation on magnesium and magnesium alloys. *Journal of Materials Science: Materials in Medicine*, 19(1), 407-415.

Poinern, G. E. J., Brundavanam, S. & Fawcett, D. (2012). Biomedical magnesium alloys: A review of material properties, surface modifications and potential as a biodegradable orthopaedic implant. *American Journal of Biomedical Engineering*, 2(6), 218-240.

Rivera-Denizard, O., Diffoot-Carlo, N., Navas, V. & Sundaram, P. A. (2008). Biocompatibility studies of human fetal osteoblast cells cultured on gamma titanium aluminide. *Journal of Materials Science: Materials in Medicine*, 19(1), 153-158.

Razavi, M., Fathi, M. H. & Meratian, M. (2010). Microstructure, mechanical properties and bio-corrosion evaluation of biodegradable AZ91-FA nanocomposites for biomedical applications. *Materials Science and Engineering, A*, 527(26), 6938-6944.

Reifenrath, J., Bormann, D. & Meyer-Lindenberg, A. (2011). Magnesium alloys as promising degradable implant materials in orthopaedic research. *Magnesium alloys—corrosion and surface treatments*, 94-108.

Revie, R. W. (2008). Corrosion and corrosion control: An introduction to corrosion science and engineering. *John Wiley & Sons*. New York.

Schutze, M. (2000). Corrosion and environmental degradation. *Wiley-Vch*. Weinheim.

Shahba, R. A., Ghannem, W. A., El-Shenawy, A. E. S., Ahmed, A. S. & Tantawy, S. M. (2011). Corrosion and inhibition of Ti-6Al-4V alloy in NaCl solution. Int. J. Electrochem. Sci, 6(11), 5499-5509.

Sul, Y. T., Johansson, C. B., Jeong, Y. & Albrektsson, T. (2001). The electrochemical oxide growth behaviour on titanium in acid and alkaline electrolytes. *Medical Engineering & Physics*, 23(5), 329-346.

Tan, Y. M. & Revie, R. W. (2012). Heterogeneous electrode processes and localized corrosion 13. *John Wiley & Sons*. New York.

Topcu, İ. (2020). Investigation of wear behavior of particle reinforced AL/B4C composites under different sintering conditions. *Tehnički glasnik*, 14(1), 7-14.

Topcu, İ., Gulsoy, H. O. & Gulluoglu, A. N. (2019). Evaluation of Multi-Walled CNT particulate reinforced Ti6Al4V alloy based composites creep behavior of materials under static loads. *Gazi University Journal of Science*, 32(1), 286-298.

Uchi, H., Kanno, T. & Alwitt, R. S. (2001). Structural features of crystalline anodic alumina films. *Journal of the Electrochemical Society*, 148(1), B17-B23.

Üner, İ. & Koçak, E.D. (2012). Poli (laktik asit)'in kullanım alanları ve nano lif üretimdeki uygulamaları. *İstanbul Ticaret Üniversitesi Fen Bilimleri Dergisi*, 11(22), 79-88.

Warranty, Nobelbiocarecom, (2016). Retrieved April 21, 2016 from https://www.nobelbiocare.com/us/en/footer/warranty.html

Wang, Y., Zhao, S., Li, G., Zhang, S., Zhao, R., Dong, A. & Zhang, R. (2020). Preparation and in vitro antibacterial properties of anodic coatings co-doped with Cu, Zn, and P on a Ti–6Al–4V alloy. *Materials Chemistry and Physics*, 241, 122360.

Wen, C. E., Mabuchi, M., Yamada, Y., Shimojima, K., Chino, Y. & Asahina, T. (2001). Processing of biocompatible porous Ti and Mg. *Scripta Materialia*, 45(10), 1147-1153.

Willert, H. G., Brobäck, L. G., Buchhorn, G. H., Jensen, P. H., Köster, G., Lang, I., Ochsner P. & Schenk, R. (1996). Crevice corrosion of cemented titanium alloy stems in total hip replacements. *Clinical Orthopaedics and Related Research*, 333, 51-75.

Witte, F., Hort, N., Vogt, C., Cohen, S., Kainer, K. U., Willumeit, R. & Feyerabend, F. (2008). Degradable biomaterials based on magnesium corrosion. *Current Opinion in Solid State and Materials Science*, 12(5-6), 63-72.

Wu, S., Liu, X., Yeung, K. W., Guo, H., Li, P., Hu, T., Chung, C.Y. & Chu, P. K. (2013). Surface nano-architectures and their effects on the mechanical properties and corrosion behavior of Ti-based orthopedic implants. *Surface and Coatings Technology*, 233, 13-26.

Yerokhin, A. L., Nie, X., Leyland, A., Matthews, A. & Dowey, S. J. (1999). Plasma electrolysis for surface engineering. *Surface and Coatings Technology*, 122(2-3), 73-93.

Yilmaz, E. B., Topcu, I. & Ceylan, M., (2020). Experimental investigation on mechanical properties of Multi Wall Carbon Nanotubes (MWCNT) reinforced aluminium metal matrix composites. *Journal of Ceramic Processing Research*, 21(5), 596-601.

Yun, Y., Dong, Z., Lee, N., Liu, Y., Xue, D., Guo, X. & Sundaramurthy, S. (2009). Revolutionizing biodegradable metals. *Materials Today*, 12(10), 22-32.

Zaffora, A., Di Franco, F., Virtù, D., Carfì Pavia, F., Ghersi, G., Virtanen, S. & Santamaria, M. (2021). Tuning of the Mg Alloy AZ31 Anodizing Process for Biodegradable Implants. *ACS applied materials & interfaces*, 13(11), 12866–12876.

Zeng, R., Dietzel, W., Witte, F., Hort, N. & Blawert, C. (2008). Progress and challenge for magnesium alloys as biomaterials. *Advanced Engineering Materials*, 10(8), B3-B14.

Zhang, E., Yin, D., Xu, L., Yang, L. & Yang, K. (2009). Microstructure, mechanical and corrosion properties and biocompatibility of Mg–Zn–Mn alloys for biomedical application. *Materials Science and Engineering: C*, 29(3), 987-993.